

QUASI-GASDYNAMIC HETEROGENEOUS MODEL FOR MODELING A MIXTURE OF COMPRESSIBLE FLUIDS

ISMATOLLO R. KHAYTALIEV^{*}, EVGENY V. SHILNIKOV^{†*} AND TATIANA G.
ELIZAROVA[†]

^{*} Moscow Automobile and Road Construction State Technical University
Leningradsky Ave., 125319 Moscow, Russia
e-mail: ikhaitaliev@gmail.com

[†] Keldysh Institute of Applied Mathematics Russian Academy of Sciences
Miuskaya sq., 4, 125047 Moscow, Russia
email: evvlash@mail.ru, telizar@mail.ru

Key words: Heterogeneous two-fluid mixture, Four-equation model, Regularized equations, Finite difference algorithm.

Summary. Quasi-gasdynamic type regularization is presented for a heterogeneous model of a two-fluid mixture of compressible fluids. This model allows to describe the flows of stiffened gases. The reduced four-equation model for dynamics of the heterogeneous compressible two-fluid mixture with equations of state of a stiffened gas is considered. A further reduced form of this model with the excluded volume concentrations and a quadratic equation for the common pressure of the components can be called a quasi-homogeneous form. A finite difference algorithm is used, built with the finite volume method. By solving one and two-dimensional test problems it is shown that the presented algorithm is a stable and reliable way to model fluid mixtures with strong shock waves.

1 INTRODUCTION

As a rule, for numerical simulations of mixture flows homogeneous or heterogeneous models are used. In the homogeneous approaches is assumed that the components of the mixture do not have pronounced boundaries and their own volumes. In this case, the pressure in the mixture is calculated as the sum of the partial pressures of the components. In the heterogeneous approaches each component of the mixture occupies its own volume. In this case, the pressure in the mixture is calculated using the equations of state of the components and their volume fractions in the mixture. Numerical experience shows that the field of applicability of the heterogeneous model is wider than the homogeneous one. In particular, on the basis of a heterogeneous model, it is possible to simulate not only gas mixtures, but also gas-liquid mixtures in the approximation of the so-called "stiffened" gas, which is essential for practical applications.

Two-fluid flows arise in various engineering applications. Examples of such flows are:

- the flow of air and water vapor in a humid environment;
- air-hydrogen flow, found in fuel cell systems or in gas transportation and storage;

- air-CO₂ flow, for example, in industrial processes or gas exchange systems;
- air-natural gas flow occurring in heaters powered by natural gas or in gas turbines.

Heterogeneous compressible mixture models differ in the number of equations included in the system - from 4 to 7 PDE's. In the seven-equation model by Baer-Nunziata [1] each component is described by its own velocity, temperature and pressure. However, for many applications, the physics included in this model is superfluous. Therefore, various lightened models are proposed, for example, a model of six equations with equilibrium velocity [2], a model with total pressure [3–4], a model of five equations with equilibrium velocity and pressure [5] and a model of four equations with equilibrium velocity, pressure and temperature.

2 QUASI-HOMOGENEOUS FORM FOR HETEROGENEOUS MIXTURE

Among the large number of algorithms for numerical simulation of the homogeneous mixture, here we will focus on the method based on regularized or quasi-gas dynamic equations [6]. These equations employ a single-temperature and single-velocity approximations of a mixture flow.

In [7], a model of heterogeneous compressible two liquid mixture with four equations and a state equation of a stiffened gas is presented. It also presents the development of a model with excluded volume concentrations and a quadratic equation for the total pressure of the components. This variant is called a quasi-homogeneous form of the heterogeneous model. It is this model that we use to build a finite difference approximation and to solve test problems.

A quasi-homogeneous system of four equations for a heterogeneous compressible two-liquid mixture with one velocity and one temperature consists of balance equations for the mass of components, total momentum and total energy:

$$\frac{\partial(\alpha_k r_k)}{\partial t} + \text{div}(\alpha_k r_k \mathbf{u}) = 0, \quad k = 1, 2, \quad (1)$$

$$\frac{\partial(\rho \mathbf{u})}{\partial t} + \text{div}(\rho \mathbf{u} \otimes \mathbf{u}) + \nabla p = \text{div} \Pi^{\text{NS}} + \rho \mathbf{f}, \quad (2)$$

$$\frac{\partial}{\partial t} (0.5 \cdot \rho |\mathbf{u}|^2 + \rho \varepsilon) + \text{div} \left((0.5 \cdot \rho |\mathbf{u}|^2 + \rho \varepsilon + p) \mathbf{u} \right) = \text{div} (-\mathbf{q}^{\text{F}} + \Pi^{\text{NS}} \cdot \mathbf{u}) + \rho \mathbf{u} \cdot \mathbf{f} + Q. \quad (3)$$

Here, r_k – the densities α_k – the volume fraction of the k -component, \mathbf{u} – the velocity and p – the pressure of the mixture. \mathbf{f} and Q denote the external force and the external source or drain of energy, respectively. The following additional ratios are used:

$$\sum_{k=1}^2 \alpha_k = 1, \quad \rho = \sum_{k=1}^2 \alpha_k r_k, \quad \rho \varepsilon = \sum_{k=1}^2 \alpha_k r_k \varepsilon_k(r_k T), \quad p = p_k(r_k T) > 0. \quad (4)$$

We apply the equations of state of a stiffened gas in the form [5,7,8]

$$p_k(r_k T) = R_k r_k T - p_{*k}, \quad \varepsilon_k(r_k T) = c_{V_k} T + \frac{p_{*k}}{r_k} + \varepsilon_{0k}. \quad (5)$$

This approximation is based on the simplified Van der Waals equation for the liquid component. The ideal polytropic case corresponds to $p_{*k} = \varepsilon_{0k} = 0$.

To exclude the values α_k and r_k from the continuity equation we introduce an alternative

density for the k -th component $\rho_k = \alpha_k r_k$. Using the previous equations, we have:

$$\sum_{k=1}^2 \frac{R_k \rho_k}{p + p_{*k}} T = 1, \quad \rho \cdot (\varepsilon - \varepsilon_0) = \left(\rho \cdot c_V + \sum_{k=1}^2 \frac{R_k \rho_k p_{*k}}{p + p_{*k}} \right) T, \quad \rho \cdot c_V = \sum_{k=1}^2 \rho_k c_{Vk}. \quad (6)$$

The last equations lead to the equation connecting pressure, densities and internal energy:

$$\sum_{k=1}^2 \frac{\sigma_k (\rho \cdot (\varepsilon - \varepsilon_0) - p_{*k})}{p + p_{*k}} = 1, \quad \sigma_k = \frac{R_k \rho_k}{c_V \cdot \rho}. \quad (7)$$

This rational equation reduces to a quadratic equation for pressure

$$p^2 - bp - c = 0 \quad (8)$$

with the coefficients

$$b = \sum_{k=1}^2 (\sigma_k (\rho \cdot (\varepsilon - \varepsilon_0) - p_{*k}) - p_{*k}), \quad c = (\sigma_1 p_{*2} + \sigma_2 p_{*1}) \cdot \rho \cdot (\varepsilon - \varepsilon_0) - \gamma \cdot p_{*1} \cdot p_{*2}. \quad (9)$$

If at least one of $p_{*k} = 0$ (only such a case is considered in this paper), the discriminant of this equation is positive and $c > 0$. Thus, the positive root of this equation gives the pressure and the negative root is discarded as non-physical.

The temperature T can be obtained from (8), and sound speed is calculated according to [7]

$$T = \left(\sum_{k=1}^2 \frac{R_k \rho_k}{p + p_{*k}} \right)^{-1}, \quad c_s^2 = \frac{\gamma}{\rho} \left(\sum_{k=1}^2 \frac{\sigma_k \cdot (\rho \cdot (\varepsilon - \varepsilon_k) - p_{*k})}{(p + p_{*k})^2} \right)^{-1}. \quad (10)$$

The approaches used in the homogeneous and heterogeneous models of gas mixtures are significantly different. However, the variant used here to describe a heterogeneous mixture formally differs from the homogeneous variant only by calculating the pressure and temperature of the mixture as well as the speed of sound in it. Namely, here the pressure is calculated according to (8), and when describing the mixture in a homogeneous approximation [9], the pressure of the mixture is calculated as the sum of the partial pressures of the components. Therefore, the above method of describing a heterogeneous mixture is promising from the point of view of its implementation in numerical algorithms already created based on a homogeneous approach.

3 REGULARIZED EQUATIONS FOR GAS MIXTURE

The regularized system of equations for describing the flow of two gases is presented in, e.g., [7 - 9]

$$\frac{\partial(\rho_k)}{\partial t} + \operatorname{div}(\rho_k (\mathbf{u} - \hat{\mathbf{w}})) = \nabla \cdot (\tau \mathbf{u} \cdot \operatorname{div}(\rho_k \mathbf{u})), \quad (11)$$

$$\frac{\partial(\rho \mathbf{u})}{\partial t} + \operatorname{div}(\rho (\mathbf{u} - \mathbf{w}) \otimes \mathbf{u}) + \nabla p = \operatorname{div} \Pi + (\rho - \tau \operatorname{div}(\rho \mathbf{u})) \mathbf{f}, \quad (12)$$

$$\frac{\partial E}{\partial t} + \operatorname{div}((E + p)(\mathbf{u} - \mathbf{w})) = -\operatorname{div} \mathbf{q} + \operatorname{div}(\Pi \cdot \mathbf{u}) + \rho (\mathbf{u} \cdot \mathbf{w}) \cdot \mathbf{f} + Q. \quad (13)$$

The auxiliary QGD quantities are small additions to the velocity, viscous stress tensor, and heat flux and have the form:

$$\begin{aligned}
 \mathbf{w}_k &= \frac{\tau}{\rho_k} \operatorname{div}(\rho_k (\mathbf{u} - \mathbf{w}) \otimes \mathbf{u}) + \hat{\mathbf{w}}, \quad \hat{\mathbf{w}} = \frac{\tau}{\rho} (\rho (\mathbf{u} \nabla) \mathbf{u} + \nabla p - \rho \mathbf{f}), \\
 \mathbf{w} &= \sum_k^2 \frac{\rho_k}{\rho} \mathbf{w}_k = \frac{\tau}{\rho} (\operatorname{div}(\rho (\mathbf{u} - \mathbf{w}) \otimes \mathbf{u}) + \nabla p - \rho \mathbf{f}), \\
 \mathbf{q} &= \mathbf{q}^{\text{NS}} + \mathbf{q}^\tau, \quad -\mathbf{q}^\tau = \tau \rho \mathbf{u} \left(\mathbf{u} c_V \nabla T + \rho (\mathbf{u} \nabla) \left(\frac{1}{\rho} \right) - \frac{Q}{\rho} \right), \\
 \Pi &= \Pi^{\text{NS}} + \rho \mathbf{u} \otimes \hat{\mathbf{w}} + \tau (\mathbf{u} \nabla p + \gamma \rho \operatorname{div}(\mathbf{u}) - (\gamma - 1) Q).
 \end{aligned} \tag{14}$$

This system differs from the classical Navier-Stokes equations by regularizing terms containing a time-factor $\tau = \alpha h/c$, where h is the spatial mesh size and c is the speed of sound in the mixture, α is a tuning numerical coefficient. In solving the Euler equations, the viscosity μ and the thermal conductivity κ of the mixture are treated as artificial regularizers and are computed using τ as

$$\mu = \tau p \text{Sc}, \quad \kappa = \frac{\mu c_p}{\text{Pr}}. \tag{15}$$

Thus, there are three free numerical parameters for tuning the dissipation properties of the algorithm: the coefficient α , the Schmidt number Sc , and the Prandtl number Pr . The baseline values are $\alpha = 0.5$ and $\text{Sc} = \text{Pr} = 1$. It is assumed that the external force \mathbf{f} and the heat source Q are equal to zero in our test problems.

A time-explicit conditionally stable difference scheme with a second order approximation in space was used. It is constructed by the finite volume method on rectangular grid. All gas dynamic variables are assigned to the centers of the cells. Their values at the cell boundaries are calculated as half-sums of values in neighboring cells. Spatial derivatives at cell boundaries are calculated using central differences. The time step is calculated using the Courant-type condition

$$\Delta t = \beta \cdot \min_i \frac{h}{c_i + |u_i|}. \tag{16}$$

Note that the additional dissipation of the scheme is strongly nonlinear and depends substantially on the local time-depending gas dynamic parameters, see (14), automatically adjusting to it.

4 1D TEST PROBLEMS

We present the results of two numerical experiments for modeling 1D shock wave flows in Euler approximation, taken from [7]. The Schmidt and the Prandtl numbers here are set equal to 1.

Problem A. We take a 1 m long tube filled with a mixture of water and water vapor with mass fraction of the vapor equals to 0.8 in the entire tube. The initial conditions are as follows:

(17)

$$(p, u, T)_1 = \left(2 \cdot 10^5 \text{ Pa}, 0 \frac{\text{m}}{\text{s}}, 394.2489 \text{ K} \right), \quad x \leq 0;$$

$$(p, u, T)_2 = \left(10^5 \text{ Pa}, 0 \frac{\text{m}}{\text{s}}, 372.8827 \text{ K} \right), \quad x > 0.$$

Table 1: Stiffened gas parameters

Substance	γ	$c_v, \text{J}/(\text{kg K})$	p_*, Pa	$\varepsilon_0, \text{J}/\text{kg}$
Water vapor	1.43	1040	0	$2030 \cdot 10^3$
Water	2.35	1816	10^9	$-1167 \cdot 10^3$

Different spatial grids, α values and Courant numbers are used. Results are shown in Figure 1 for $t_{fin} = 0.8$ ms.

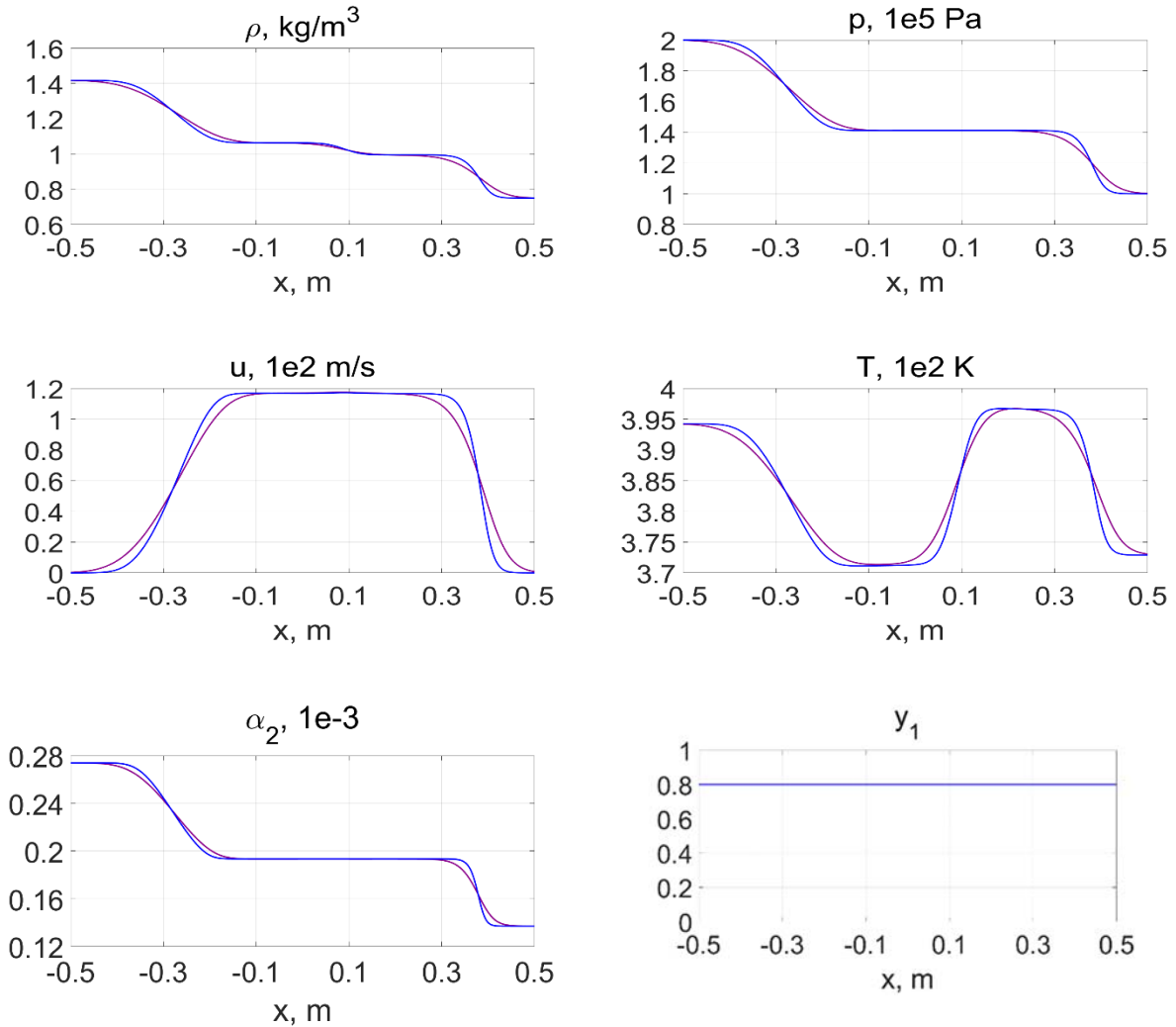


Figure 1: Numerical solutions at $\alpha = 0.8$. Number of grid points N . Dark purple $N = 2000$; Blue $N = 5000$

Presented here distributions show the total density of the mixture, as well as the volume fraction of the liquid phase, pressure p , velocity u and the absolute temperature T of the mixture. N is the number of grid cells. It is seen that on a more detailed grid the solution is better, that confirms the convergence of the numerical results.

Figure 1 shows a comparison of numerical solutions at $\alpha = 0.8$ for a different number of N points. It is shown that increasing the number of points N makes the solution less smooth. Note, that Figure 1 (b) shows the water concentration profile α_2 .

Figure 2 presents the calculation results for different values of parameter α . It is seen that reducing α leads to an improvement in the quality of the solution.

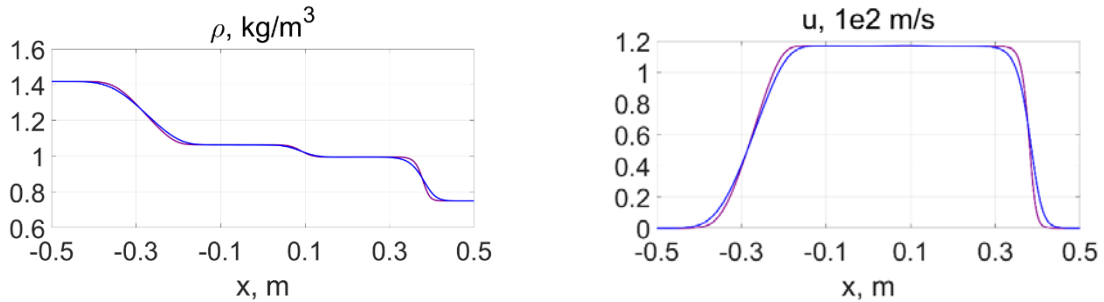


Figure 2: Comparison of numerical solutions for density and velocity at $N = 5000$ for different values of α . Dark purple $\alpha = 0.4$; Blue $\alpha = 0.8$

Problem B. Here, we simulate depressurization of a 160-m long pipe ($-80 < x < 80$) that is filled with pure carbon dioxide. The pipe is filled with liquid carbon dioxide at the left, and with the gas carbon dioxide at the right. The initial conditions are:

$$\begin{aligned} (p, u, T)_1 &= \left(6 \cdot 10^5 \text{ Pa}, 0 \frac{\text{m}}{\text{s}}, 283.13 \text{ K} \right), \alpha_1 = 0, x \leq 10; \\ (p, u, T)_2 &= \left(10^6 \text{ Pa}, 0 \frac{\text{m}}{\text{s}}, 283.13 \text{ K} \right), \alpha_1 = 1, x > 10. \end{aligned} \quad (18)$$

Table 2: Stiffened gas parameters

Substance	γ	$c_v, \text{J}/(\text{kg K})$	p_*, Pa	$\varepsilon_0, \text{J}/\text{kg}$
Vapor	1.06	2410	$9.86 \cdot 10^5$	$-3.01 \cdot 10^3$
Liquid	1.23	2440	$1.32 \cdot 10^8$	$-6.23 \cdot 10^3$

Results at $t_{fin} = 80$ ms are shown in Figure 3. Different spatial grids, values of regularization parameter α and Courant number $\beta = 0.1$ are used. Here are the distributions of the same quantities as for the previous problem, except vapor concentration profile α_1 . Here also the increasing the number of points N makes the solution less smooth.

Figure 4 shows the comparison of numerical solutions for temperature and velocity at different parameters α . A mesh with 1200 elements is used. It is also seen here that with lower values of α , the fronts turn out to be steeper.

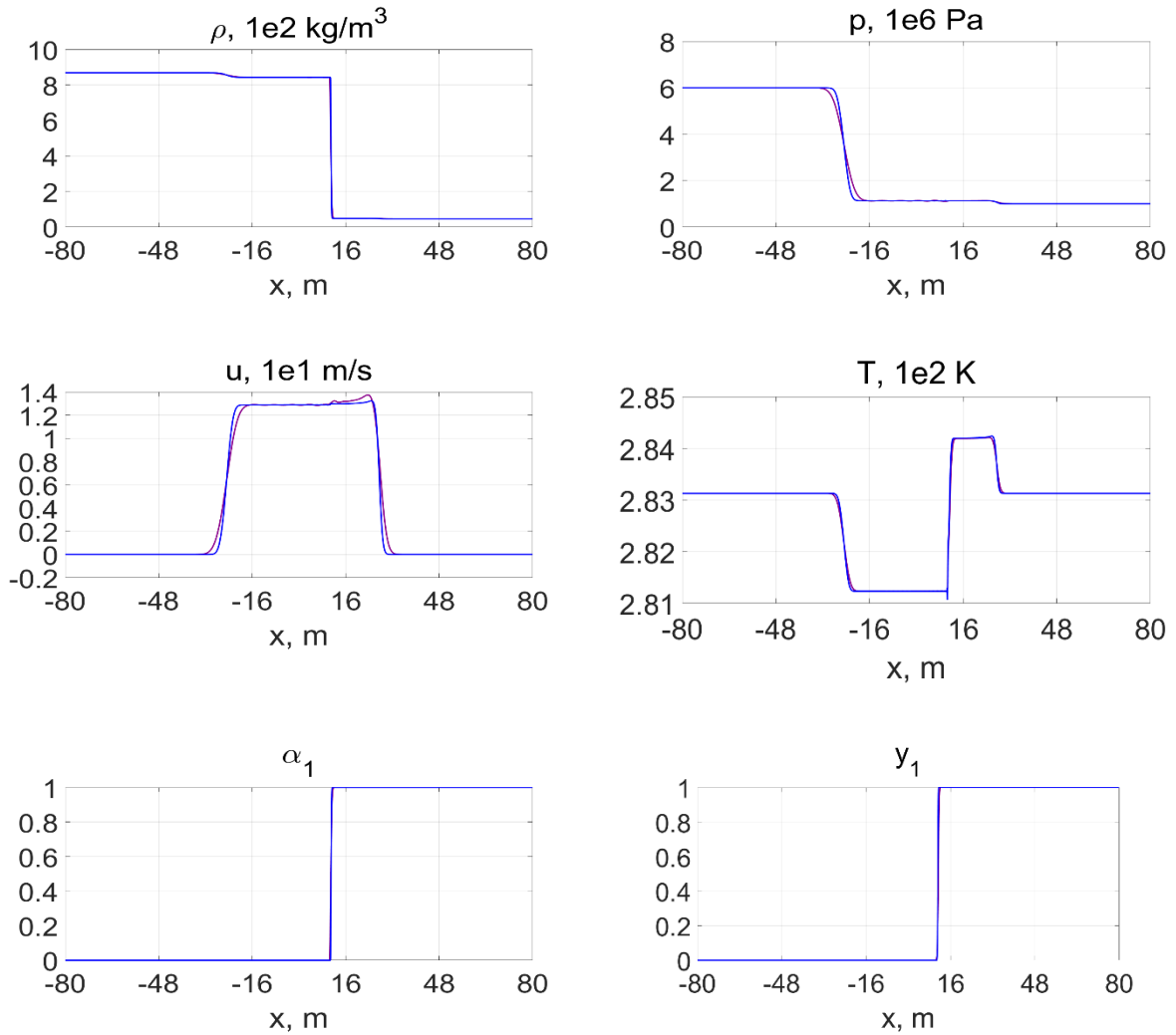


Figure 3: Numerical solutions at $\alpha = 0.8$ for a different N . Dark purple $N = 1200$; Blue $N = 4000$

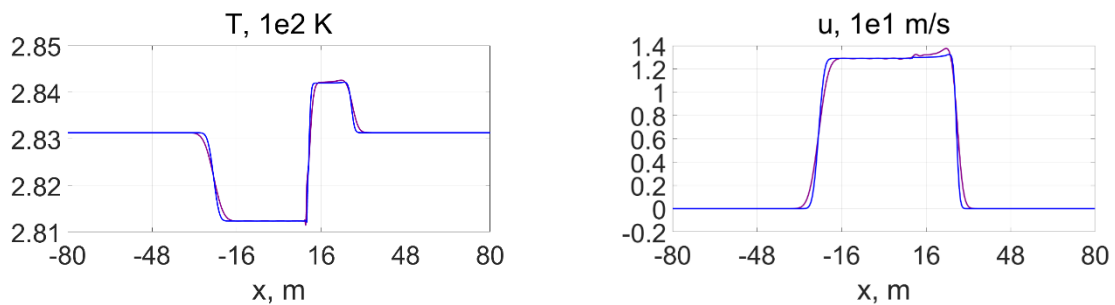


Figure 4: Comparison of numerical solutions for temperature and velocity at $N = 1200$ for different values of α . Dark purple $\alpha = 0.4$; Blue $\alpha = 0.8$

5 2D TEST PROBLEMS

Here we present the results of two numerical experiments for modeling shock wave flows. The problem statements are taken from [7] for the air and water medium. The calculation area is $x \in [-15 \text{ mm}, 25 \text{ mm}]$ and $y \in [0 \text{ mm}, 15 \text{ mm}]$. The cylindrical water drop with radius $r = 3.2 \text{ mm}$ is centered at $(0, 0)$.

Since this problem is symmetric with respect to the X -axis, the flow around only the upper half of the drop is simulated, and the symmetry condition is imposed on the lower boundary. Input conditions are set on the left boundary and output conditions – on the right one. The slip conditions are set on the upper wall. These boundaries are located far enough from the drop.

The parameters of the fluids used in these tasks are

Table 3: The parameters of the fluids

Substance	γ	$c_p, \text{J}/(\text{kg K})$	p_*, Pa	$\varepsilon_0, \text{J/kg}$
1. Air	1.4	1004.5	0	0
2. Water	2.8	4186	$8.5 \cdot 10^8$	0

We use Schmidt number $Sc = 1$, Prandtl number $Pr = 1$ and Courant number $\beta = 0.1$. Different spatial grids and values of parameter α are used.

A smooth transition of the volume fraction at the interface of the droplet is necessary. A width of $\pm 2 \cdot h_x$ is used for the transition region [5]. This transition is given by the following formula:

$$\begin{aligned}
(\alpha_1)_{\text{blended}} &= G(\xi) \cdot \varepsilon + (1 - G(\xi)) \cdot (1 - \varepsilon), \\
G(\xi) &= -\xi^2 (2\xi - 3), \\
\xi &= \frac{(x^2 + y^2)^{0.5} - (r - 2h_x)}{4h_x}, \quad r - 2h_x \leq (x^2 + y^2)^{0.5} \leq r + 2h_x
\end{aligned} \tag{19}$$

Problem C. A shock wave in air impacting a water column (i.e., 2D droplet) is simulated. The initial conditions are as follows: air in whole region with the following parameters:

$$\begin{aligned}
(p, \alpha, u_x, u_y, T)_L &= (2.35438 \cdot 10^5 \text{ Pa}, \varepsilon, 225.86 \text{ m/s}, 0 \text{ m/s}, 381.85 \text{ K}) \text{ for } x \leq -4 \text{ mm}; \\
(p, \alpha, u_x, u_y, T)_R &= (1 \cdot 10^5 \text{ Pa}, \varepsilon, 0 \text{ m/s}, 0 \text{ m/s}, 293.15 \text{ K}) \text{ for } x > -4 \text{ mm}, \\
&\text{except for } x^2 + y^2 < r^2, \text{ where } \alpha = 1 - \varepsilon \text{ and } \varepsilon = 1 \cdot 10^{-5} \text{ (water)}.
\end{aligned} \tag{20}$$

The results are presented in Figure 5. Pressure profiles are shown at $t = 6.25 \mu\text{s}$, $t = 6.75 \mu\text{s}$ and $t = 18.75 \mu\text{s}$. The uniform grid 1400×600 is used. Regularization parameter $\alpha = 0.8$.

It can be seen that the shape of the water droplet practically does not change under the influence of the shock wave.

The numerical Schlieren function is computed as exponential distribution of ‘Density Gradient Magnitude’. We use reverse grayscale color map with 100 levels. For problem C $\min = 5$, $\max = 1.25 \cdot 10^7$, for problem D $\min = 10^4$, $\max = 10^7$.

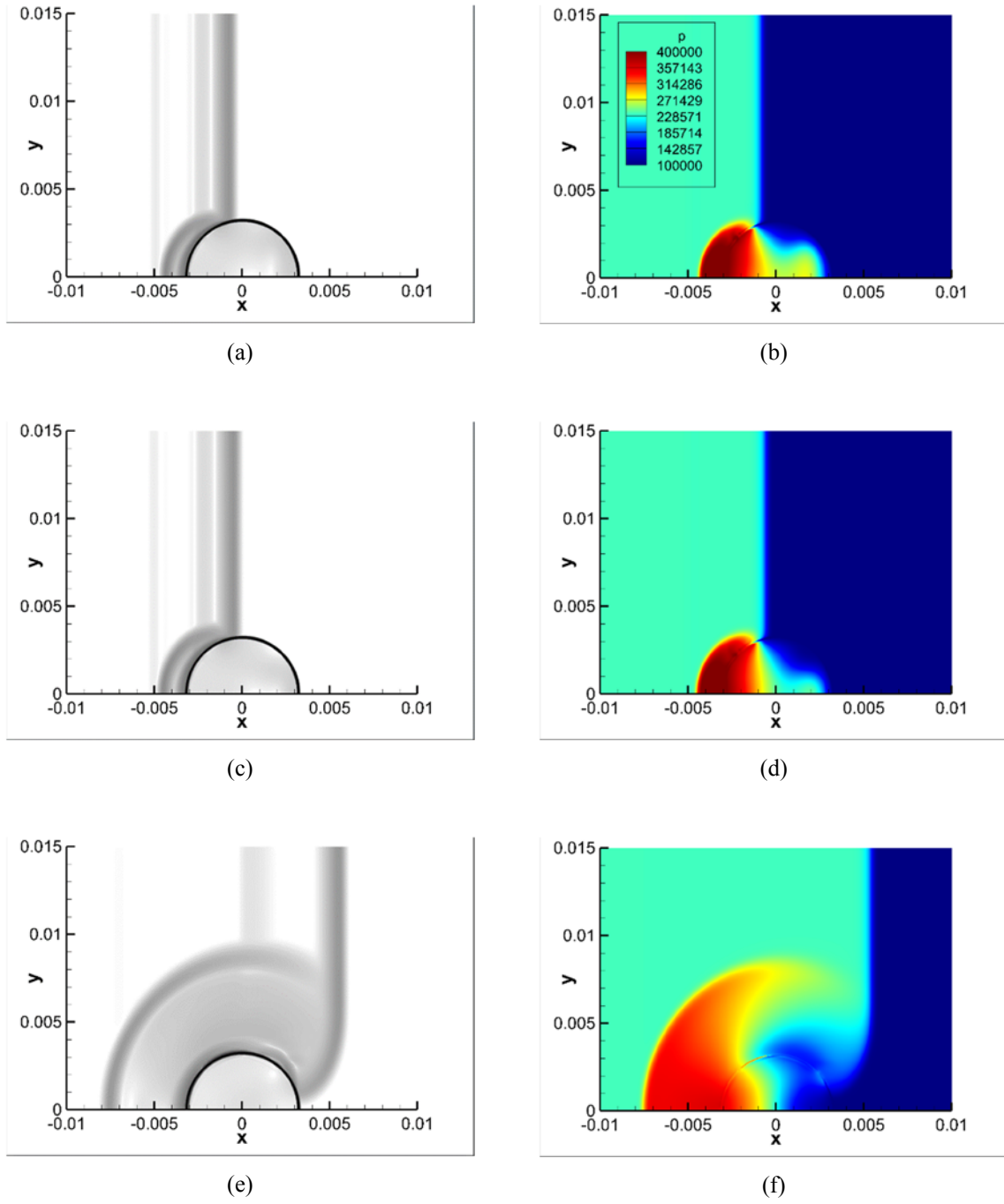


Figure 5: Task C. Numerical solutions at different time points on the 1400×600 grid for $\alpha = 0.8$: (a) $t = 2.5 \mu\text{s}$ (numerical Schlieren); (b) $t = 2.5 \mu\text{s}$ (pressure); (c) $t = 3.75 \mu\text{s}$ (numerical Schlieren); (d) $t = 3.75 \mu\text{s}$ (pressure); (e) $t = 5.0 \mu\text{s}$ (numerical Schlieren); (f) $t = 5.0 \mu\text{s}$ (pressure)

Problem D. This test is opposite to the previous one, with a water shock impacting a column of an air bubble, but with a much higher pressure ratio ($p_1/p_2 = 1.6 \cdot 10^4$). The initial conditions are as follows: water in whole region with the following parameters:

$$\begin{aligned} (p, \alpha, u_x, u_y, T)_L &= (1.6 \cdot 10^9 \text{ Pa}, 1 - \varepsilon, 661.81 \text{ m/s}, 0 \text{ m/s}, 593.13 \text{ K}) \text{ for } x \leq -4 \text{ mm}; \\ (p, \alpha, u_x, u_y, T)_R &= (1.01325 \cdot 10^5 \text{ Pa}, 1 - \varepsilon, 0 \text{ m/s}, 0 \text{ m/s}, 292.98 \text{ K}) \text{ for } x > -4 \text{ mm}, \\ &\text{except for } x^2 + y^2 < r^2, \text{ where } \alpha = \varepsilon \text{ and } \varepsilon = 1 \cdot 10^{-3} \text{ (air)}. \end{aligned} \quad (21)$$

The results are shown in Figure 6. Pressure profiles are demonstrated at $t = 2.5 \mu\text{s}$, $t = 3.75 \mu\text{s}$ and $t = 5 \mu\text{s}$. The uniform grid 1400×600 is used. This calculation was carried out with $\alpha = 0.4$ up to the moment $t = 3.8$ microseconds, after which it was necessary to increase it up to 1.1. Without this, at the moment of collapse of the air bubble, the solution crashed.

The shock wave, upon reaching the bubble, is partially reflected back into the water, forming a rarefaction wave that travels in the opposite direction. Rest of the shock wave is transmitted into the air bubble. The bubble is noticeably deformed. At $t = 3.75 \mu\text{s}$, the bubble's deformation reaches a point where it collapses upon itself. Following this deformation, the air within the separated bubbles is further compressed as the flow progresses. Beyond this point, the bubble appears to be completely dissipated. A higher resolution mesh would be required to investigate the details beyond this point. Nonetheless, despite the bubble's deformation and collapse, the numerical algorithm maintains its stability.

Here, the waves turned out to be thinner than in the previous calculation due to the lower value of α . The convergence of the algorithm over the grid was studied.

Test problems simulations demonstrate the reliability of the approach used with the correct selection of parameters. The calculation results are in good agreement with the calculations of other authors and for more complex models and algorithms. The algorithm is constructed in a form convenient for subsequent implementation into the OpenFOAM open software package, as an addition to the homogeneous gas mixture model based on regularized gas dynamic equations already included in this package complex.

12 CONCLUSIONS

Quasi-gasdynamic regularization is presented for a heterogeneous model of a compressible mixture flow. The homogeneous gas model was modified to construct heterogeneous simplified model consisting of four equations with equations of state of a stiffened gas. This model with excluded volume concentrations and a quadratic equation for the total gas pressure has a quasi-homogeneous form. This model was realized by numerical algorithm with central difference approximations of all spatial derivatives. The solving of 1D and 2D test problems shows that the presented algorithm is a reliable way to simulate the flows of heterogeneous mixtures with shock waves. The algorithm is constructed in a form convenient for subsequent implementation into the OpenFOAM open software package, as an addition to the homogeneous gas mixture model already included in this complex.

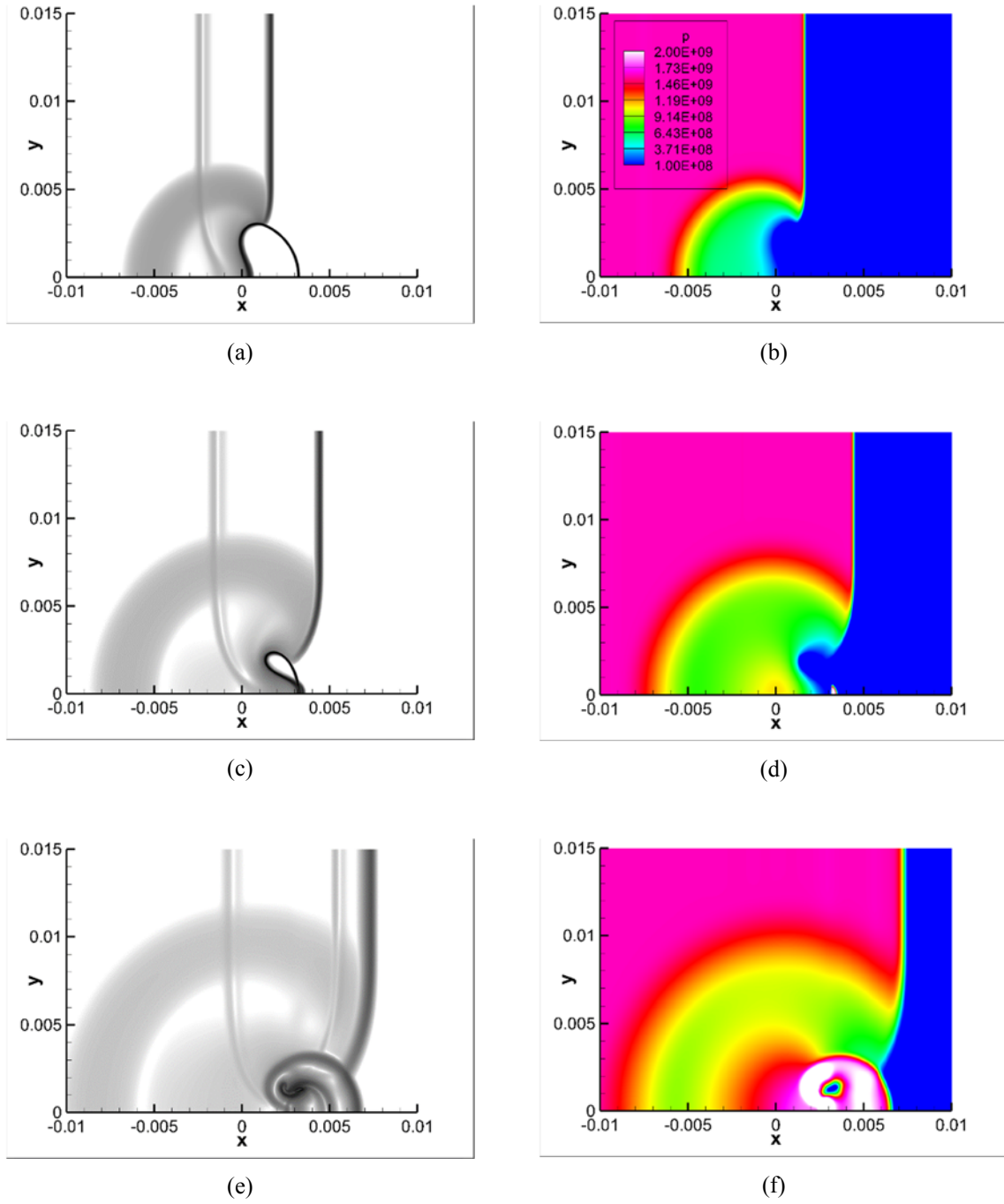


Figure 6: Task D. Numerical solutions at different time points on the 1400×600 grid: (a) $t = 2.5 \mu\text{s}$ (numerical Schlieren); (b) $t = 2.5 \mu\text{s}$ (pressure); (c) $t = 3.75 \mu\text{s}$ (numerical Schlieren); (d) $t = 3.75 \mu\text{s}$ (pressure); (e) $t = 5.0 \mu\text{s}$ (numerical Schlieren); (f) $t = 5.0 \mu\text{s}$ (pressure)

REFERENCES

- [1] M.R. Baer, J.W. Nunziato. A two-phase mixture theory for the deflagration-to-detonation transition (ddt) in reactive granular materials // *International Journal of Multiphase Flow*. 1986. Vol. 12, Is. 6. P. 861–889. ISSN 0301-9322. [https://doi.org/10.1016/0301-9322\(86\)90033-9](https://doi.org/10.1016/0301-9322(86)90033-9)
- [2] Pelanti M., Shyue K.-M. A mixture-energy-consistent six-equation two-phase numerical model for fluids with interfaces, cavitation and evaporation waves // *Journal of Computational Physics*. 2014. Vol. 259. P. 331–357.
- [3] Pandare A.K., Luo H., Bakosi J. An enhanced AUSM+-up scheme for high-speed compressible two-phase flows on hybrid grids // *Shock Waves*. 2019. Vol. 29. P. 629–649.
- [4] Lia L., Lohner R., Pandare A.K., Luo H. A vertex-centered finite volume method with interface sharpening technique for compressible two-phase flows // *Journal of Computational Physics*. 2022. Vol. 460. 111194. <https://doi.org/10.1016/j.jcp.2022.111194>
- [5] Kitamura K., Liou M.-S., Chang C.-H. Extension and comparative study of AUSM-family schemes for compressible multiphase flow simulations // *Communications in Computational Physics*. 2014. Vol. 16. P. 632–674.
- [6] Elizarova T.G., Shil'nikov E.V. Numerical simulation of gas mixtures based on the quasi-gasdynamic approach as applied to the interaction of shock wave with a gas bubble // *Computational Mathematics and Mathematical Physics*. 2021. Vol. 61, No. 1. P. 118–128. <https://doi.org/10.1134/S0965542521010048>
- [7] Zlotnik A.A., Lomonosov T.A. On a Doubly Reduced Model for Dynamics of Heterogeneous Mixtures of Stiffened Gases, its Regularizations and their Implementations // *Chaos*. 2023. Vol. 33, No. 11. 113128. <http://doi.org/10.1063/5.0159201>
- [8] Zlotnik A.A., Lomonosov T.A., Regularized equations for dynamics of the heterogeneous binary mixtures of the Noble-Abel stiffened-gases and their application // *Doklady Mathematics*. 2023. 514:1, 26–33. <https://doi.org/10.1134/S1064562423701338>
- [9] Elizarova T.G. and Shil'nikov E.V. Quasi-Gasdynamic Model and Numerical Algorithm for Describing Mixtures of Different Fluids // *Computational Mathematics and Mathematical Physics*. 2023. Vol. 63, No. 7. P. 1319–1331. Pleiades Publishing, Ltd. <https://doi.org/10.1134/S0965542523070059>